Nanomolar CFTR Inhibition by Pore-Occluding Divalent Polyethylene Glycol-Malonic Acid Hydrazides

N.D. Sonawane,[1] Dan Zhao,[1] Olga Zegarra-Moran,[2] Luis J.V. Galietta,[2] and A.S. Verkman[1],*

[1]Departments of Medicine and Physiology, 1246 Health Sciences East Tower, University of California, San Francisco CA 94143-0521, USA
[2]Laboratorio di Genetica Molecolare, Istituto Giannina Gaslini, 16148 Genova, Italy
*Correspondence: alan.verkman@ucsf.edu
DOI 10.1016/j.chembiol.2008.05.015

SUMMARY

Inhibitors of the cystic fibrosis transmembrane conductance regulator (CFTR) chloride channel have potential application as antisecretory therapy in cholera. We synthesized mono- and divalent CFTR inhibitors consisting of a malonic acid hydrazide (MalH) coupled via a disulfonic stilbene linker to polyethylene glycols (PEGs; 0.2–100 kDa). IC_{50} values for CFTR inhibition were 10–15 μM for the monovalent MalH-PEGs, but substantially lower for divalent MalH-PEG-MalH compounds, decreasing from 1.5 to 0.3 μM with increasing PEG size and showing positive cooperativity. Whole-cell patch-clamp showed voltage-dependent CFTR block with inward rectification. Outside-out patch-clamp showed shortened single-channel openings, indicating CFTR pore block from the extracellular side. Luminally added MalH-PEG-MalH blocked by >90% cholera toxin-induced fluid secretion in mouse intestinal loops (IC_{50} ~10 pmol/loop), and greatly reduced mortality in a suckling mouse cholera model. These conjugates may provide safe, inexpensive antisecretory therapy.

INTRODUCTION

Secretory diarrheas, such as those produced by enterotoxins from *Vibrio cholerae* (in cholera) and *Escherichia coli* (in traveler's diarrhea) involve active chloride secretion by enterocytes into the intestinal lumen, creating a driving force for sodium and water secretion. Evidence from cell culture and animal models (Clarke et al., 1992; Gabriel et al., 1994; Kunzelmann and Mall, 2002; Field, 2003; Thiagarajah et al., 2003) indicate that intestinal chloride secretion in enterotoxin-mediated secretory diarrheas occurs mainly through the cystic fibrosis transmembrane conductance regulator (CFTR) protein, a chloride channel regulated by cAMP-dependent phosphorylation, which, when mutated, causes the hereditary disease cystic fibrosis (Boucher, 2004). CFTR inhibition is predicted to be of clinical benefit as antisecretory therapy in various types of diarrheas (Barrett and Keely, 2000; Li et al., 2005; Thiagarajah and Verkman, 2005), as well as in retarding cyst growth in autosomal dominant polycystic kidney disease where fluid secretion into the lumen of expanding cysts is CFTR-dependent (Li et al., 2004; Yang et al., 2008).

High-throughput screening of drug-like small molecules has yielded two classes of CFTR inhibitors with micromolar potency (Ma et al., 2002; Muanprasat et al., 2004). The thiazolidinone $CFTR_{inh}$-172 acts from the cytoplasmic side of the plasma membrane to produce a voltage-independent CFTR block in which the channel closed state is stabilized (Ma et al., 2002; Taddei et al., 2004). $CFTR_{inh}$-172 is absorbed rapidly across the intestinal wall and undergoes intestinal accumulation by an enterohepatic circulation mechanism (Sonawane et al., 2005). In rodent models, systemically administered $CFTR_{inh}$-172 blocked cholera toxin- and heat stable *E. coli* (STa) toxin-induced intestinal fluid secretion (Thiagarajah et al., 2003). Prior, less potent CFTR inhibitors, such as glibenclamide, diphenylamine-2-carboxylate, 5-nitro-2(3-phenylpropyl-amino)benzoate, and flufenamic acid, also act from the cytoplasmic side, but generally produce outwardly rectifying currents suggestive of an internal pore occlusion mechanism (Sheppard and Welsh, 1992; McCarty et al., 1993; Walsh et al., 1999; Hwang and Sheppard, 1999; Zhou et al., 2002). Recently, α-aminoazaheterocycle-methylglyoxal adducts were reported as potent CFTR inhibitors (Routaboul et al., 2007); however, through the use of several function CFTR assays, we could not confirm these findings (Sonawane et al., 2008). A second class of small-molecule CFTR inhibitors discovered in a larger screen designed to identify inhibitors with an external site of action, the glycine hydrazides, such as GlyH-101 (Figure 1A, left), produce inwardly rectifying chloride currents with rapid channel flicker, suggesting external pore occlusion (Muanprasat et al., 2004). The expression of CFTR at the lumen-facing plasma membrane in intestinal epithelium provides an opportunity to develop nonabsorbable, and therefore potentially very safe, antisecretory agents for diarrhea therapy.

To prove an external site of action for the glycine hydrazides, polyethylene glycol (PEG) conjugates of related malonic acid hydrazide (MalH) analogs were synthesized (Figure 1A, center) and found to block CFTR chloride current rapidly and fully when added to solutions bathing the external cell surface (Sonawane et al., 2006). The MalH-PEG conjugates prevented cholera toxin-induced intestinal fluid secretion when present in the lumen of closed intestinal loops in mice. However, the IC_{50} values for CFTR inhibition by MalH-PEG conjugates were generally >5 μM, and inhibition was reversed rapidly following washout, which are potential concerns for oral therapy of severe secretory diarrhea where rapid intestinal fluid transit might reduce compound activity by dilutional washout. We recently introduced a novel approach to address these concerns by MalH conjugation to lectins; the MalH-lectins had substantially improved CFTR inhibition
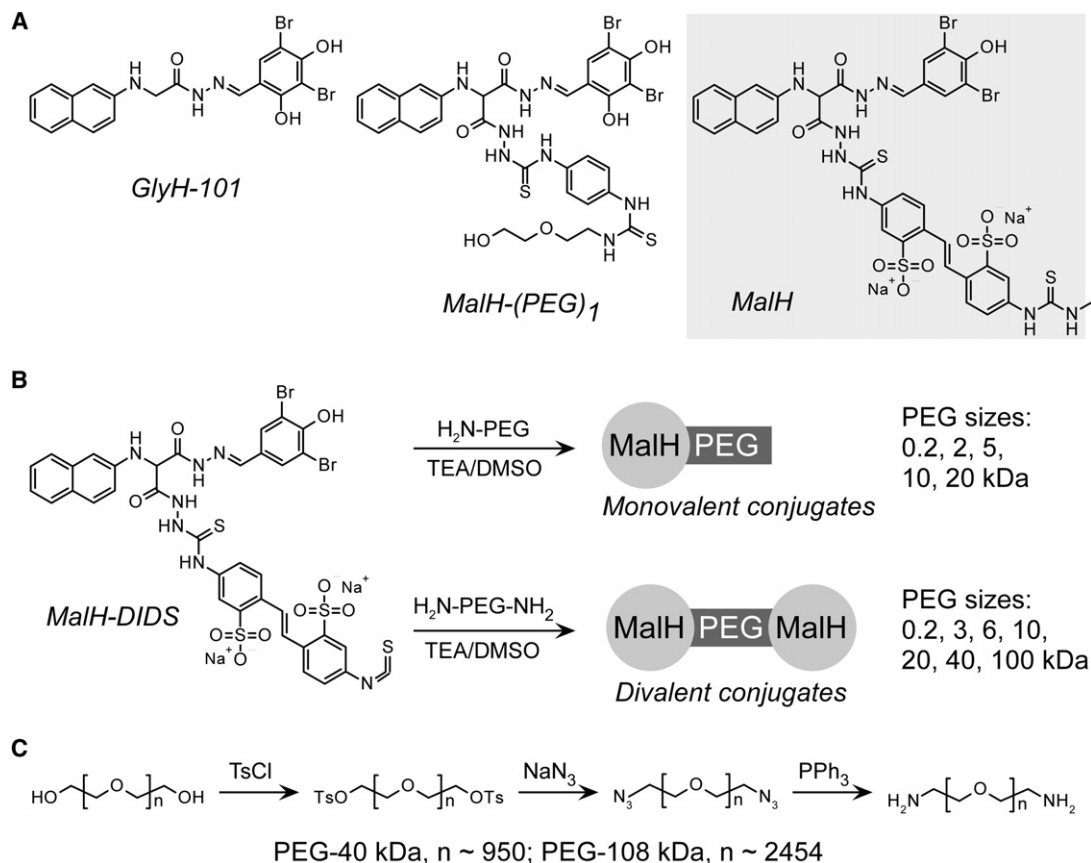
Figure 1. Synthesis of Monovalent and Divalent MalH-PEGs

(A) Structures of the GlyH-101, MalH-(PEG)$_1$, and the MalH moiety.

(B) Synthesis of MalH-PEGs. MalH-DIDS was conjugated to monoamino and bisamino PEGs to produce MalH-PEG and MalH-PEG-MalH conjugates. Reaction conditions: TEA, DMSO, room temperature, 24 hr.

(C) Synthesis of bisamino PEG 40 kD and 108 kDa. From left to right: TsCl, TEA, DCM; NaN$_3$, DMF, 40°C; PPh$_3$, H$_2$O.

potency down to 50 nM, and resisted intestinal washout because of their high affinity and entrapment in the enterocyte glycocalyx (Sonawane et al., 2007). Although effective, the relatively high cost and limited stability of protein-based therapeutics are disadvantages for use in developing countries. Here, based on the emerging paradigm of enhanced potency of multivalent ligands (Gestwicki et al., 2002; Handl et al., 2007) and evidence for CFTR channel clustering (Krouse and Wine, 2001), possibly mediated by PDZ-domain interactions (Wang et al., 2000), and evidence of dimeric/oligomeric CFTR assembly in membranes (Zerhusen et al., 1999; Ramjeesingh et al., 2003; Schillers et al., 2004), we evaluated the utility of divalent, macromolecular MalH conjugates as externally acting CFTR inhibitors. Large, divalent MalH-PEG conjugates were found to block CFTR chloride current with high potency and showed antidiarrheal efficacy in mouse models of cholera.

RESULTS

Synthesis of MalH-PEG Conjugates

As mentioned in the INTRODUCTION, we postulated that divalent compounds consisting of two CFTR inhibitor moieties sepa-

rated by a sufficiently long spacer might be substantially more potent in blocking CFTR than prior monovalent compounds. As shown in Figure 1B, the divalent (MalH-PEG-MalH) and the monovalent (MalH-PEG) conjugates were synthesized by reaction of the corresponding bisamino and monoamino PEGs with a 5-fold molar excess of MalH-DIDS in anhydrous DMSO in the presence of triethylamine as a base catalyst. Unreacted MalH-DIDS was removed by an amino-functionalized scavenger, and the PEG conjugates were purified by controlled precipitation and combinations of gel filtration, dialysis, ion exchange chromatography, and preparative HPLC.

Compound purity and absence of unreacted MalH-DIDS were confirmed by HPLC/MS, and the PEG conjugates were characterized by ^{1}H NMR, mass spectrometry, and UV/visible spectroscopy. Figure 2A provides a representative ^{1}H NMR spectrum of 20 kDa MalH-PEG-MalH, showing a prominent peak for the PEG protons and a relatively small peak in the aromatic region seen after y-scale expansion. Similar NMR spectra were obtained for the other conjugates. Mass spectra of monovalent MalH-PEG conjugates of 0.75 and 2 kDa, and a divalent MalH-PEG-MalH conjugate of 3 kDa, are provided in Figures 2B and 2C. Mass spectra confirmed the predicted molecular weights.
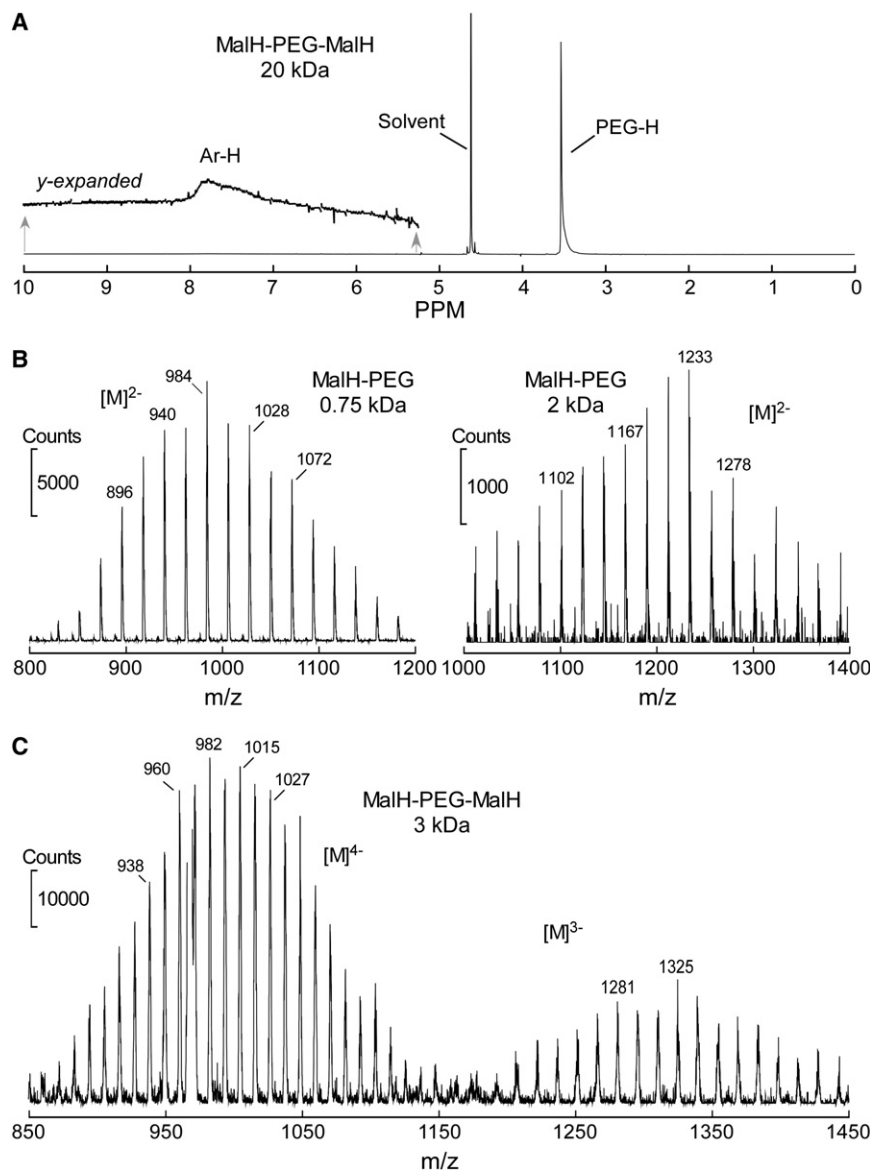
Figure 2. Characterization of MalH-PEG and MalH-PEG-MalH Conjugates

(A) ^{1}H-NMR spectrum of 20 kDa diavalent MalH-PEG-MalH conjugate showing peaks corresponding to aliphatic and aromatic protons of PEG and MalH moieties, respectively.

(B) Negative ion electrospray ionization (ESI) mass spectra of monovalent MalH-PEG conjugates of 0.75 and 2 kDa.

(C) Negative ion ESI mass spectra for 3 kDa divalent MalH-PEG-MalH conjugate showing the peaks for $[M]^{3-}$ and $[M]^{4-}$ ions with polydispersity.

Improved CFTR Inhibition of Divalent MalH-PEG-MalH Conjugates

CFTR inhibition by the MalH-PEG conjugates was measured by a fluorescence cell-based assay utilizing transfected cells expressing human wild-type CFTR and a yellow fluorescent protein (YFP) iodide sensor, as previously described (Galietta et al., 2001). CFTR-facilitated iodide influx following extracellular iodide addition results in quenching of cytoplasmic YFP fluorescence. Inhibitors were added 5 min after maximal stimulation of CFTR with a mixture of forskolin, IBMX, and apigenin. Figure 3A shows representative original fluorescence data for conjugates of 20 kDa molecular size showing substantially greater inhibition potency by the divalent (left panel) versus monovalent (right panel) conjugate. Figure 3B shows percentage CFTR inhibition, as determined from initial curve slopes, for each of the monovalent and divalent conjugates. Figure 3C summarizes IC_{50} values and Hill coefficients determined by nonlinear regression to a single-site inhibition model. Remarkably lower IC_{50}

Higher molecular weight PEG conjugates had considerable polydispersity, with the expected characteristic peak spacing of CH_2-CH_2-O = 44 Da/charge.

Bisamino-PEGs of up to 20 kDa were available commercially, giving solution lengths of up to 10 nm (Baird et al., 2003), slightly less than that estimated for the distance between CFTR pores in a potential CFTR dimer (Rosenberg et al., 2004; Riordan, 2005; Guggino and Stanton, 2006), or in tightly packed CFTR clusters. To generate larger conjugates with greater solution lengths to potentially span inhibitor binding sites in CFTR clusters, available PEGs of 40 and 108 kDa with terminal hydroxyls were converted to mesylates, followed by reaction with sodium azide and Staudinger reduction (Staudinger and Meyer 1919; Pal et al., 2004; Figure 1C). The bisamino-PEGs were confirmed by ^{1}H NMR, giving multiple peaks for CH_2-NH_2 in the range of 2.90–3.10 ppm, and ^{13}C NMR showing C-NH_2 at ~40 ppm (rather than ~60 ppm for C-OH; spectra not shown).

values were found for all divalent versus monovalent conjugates, with greater Hill coefficients, providing evidence for a cooperative mechanism for CFTR inhibition by the divalent conjugates in which both MalH moieties in a divalent conjugate interact with CFTR.

Short-circuit current measurements were done to verify the apical membrane surface site of action and relative potencies of the MalH-PEG conjugates, and to determine the kinetics of CFTR inhibition. Figures 4A and 4B show representative short-circuit current data for inhibition of CFTR-mediated apical membrane chloride current by the divalent and monovalent MalH-PEGs, respectively. The conjugates were added only to the solution bathing the apical cell surface. In general, inhibition was rapid and was near complete at higher concentrations of the conjugates. CFTR chloride current was inhibited with IC_{50} values of <1 µM for many of the divalent conjugates, whereas IC_{50} values for the monovalent conjugates were
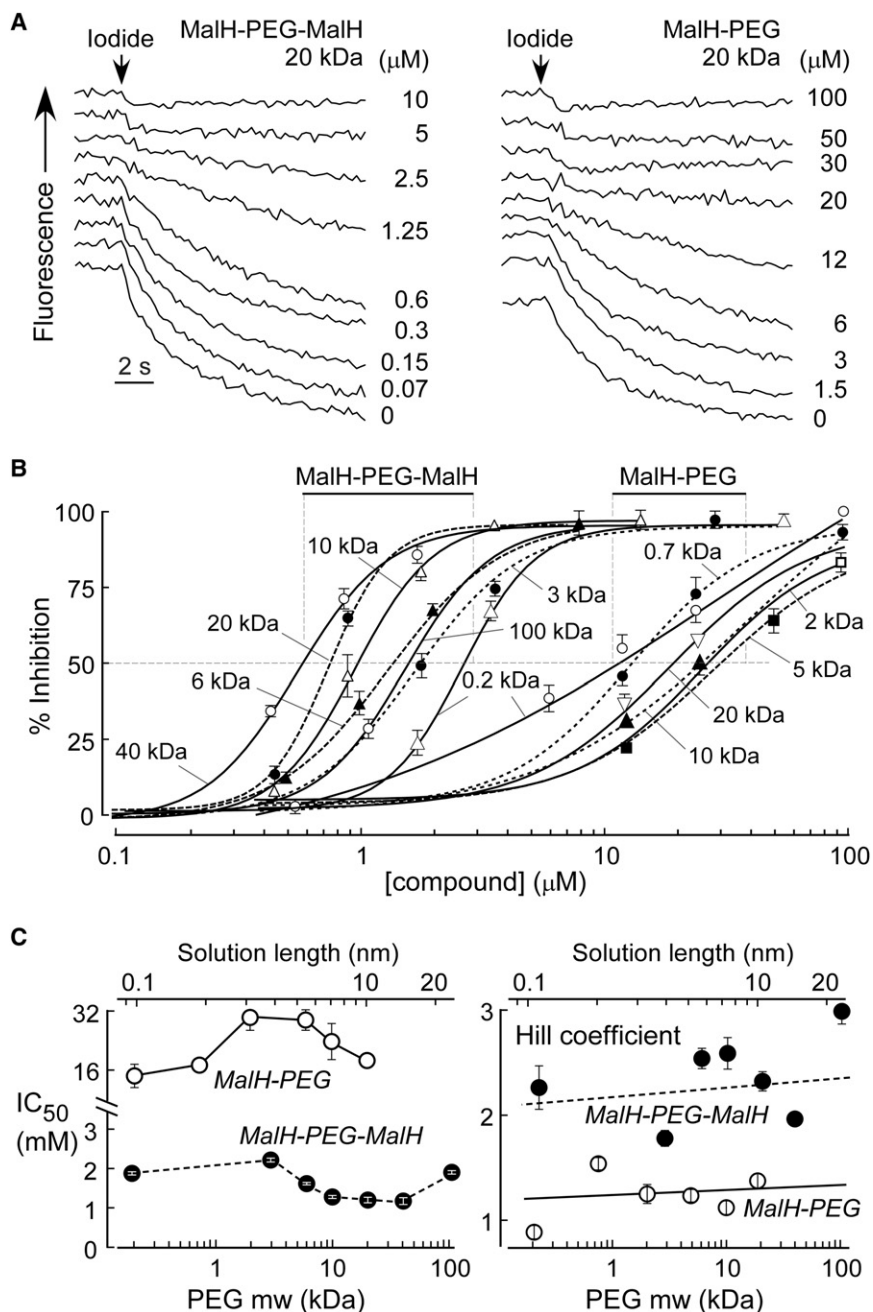
Figure 3. CFTR Inhibition by MalH-PEG Conjugates

(A) Original fluorescence assay data for CFTR inhibition by 20 kDa MalH-PEG-MalH (left) and MalH-PEG (right). CFTR was maximally stimulated by a mixture of forskolin, IBMX and apigenin in stably transfected FRT cells coexpressing human CFTR and the yellow fluorescent protein YFP-H148Q/I152L. The fluorescence decrease following iodide addition represents CFTR halide conductance.

(B) Concentration-inhibition data for indicated monovalent and divalent conjugates determined from the fluorescence assay. Error bars represent ± SE (n = 3–5). Data fitted to single-site inhibition model.

(C) Fitted IC_{50} values for monovalent and divalent conjugates as a function of molecular size, with calculated gyration radii shown (left); fitted Hill coefficients (right). At each molecular size, IC_{50} values and Hill coefficients differed significantly (p < 0.01; Student's t test). Error bars represent ± SE.

Mechanism of CFTR Inhibition by MalH-PEG Conjugates

Whole-cell patch-clamp was done to investigate the mechanism of CFTR inhibition by the MalH-PEG conjugates. Experiments were done comparing monovalent versus divalent conjugates of 20 kDa molecular size, where IC_{50} differed by >20-fold. Whole-cell CFTR chloride currents were measured in the absence of inhibitors, and at concentrations near the IC_{50} values of 0.6 and 15 μM for the divalent and monovalent conjugates, respectively. Figures 5A and 5B show representative traces, with averaged current-voltage relationships shown in Figures 5C and 5D. Both compounds produced voltage-dependent inhibition of CFTR currents, with positive currents being more strongly affected, producing inwardly rectifying behavior, which is consistent with occlusion of the channel pore. CFTR inhibition by the MalH-PEG conjugates was reversible following inhibitor washout, with recovery to baseline current in 2–4 min.

generally >10 μM (Figure 4C). These results are in general agreement with those obtained by the fluorescence assay, although exact values differ because of differences in assay conditions, such as differences in apical membrane potential and dilution effects in the fluorescence assay. In both assays, IC_{50} values of the divalent compounds decreased with increasing molecular size, except for the largest compound (100 kDa). The size-dependent inhibition potency is likely the consequence of several factors, including inhibitor steric access to its binding site, the energetics and location of the MalH binding site(s), and the conformational entropy of the PEGs.

The CFTR current traces at different membrane potentials revealed slow channel block by the MalH-PEG conjugates. When membrane voltage was clamped from a holding potential of 0 mV to a positive or a negative potential, CFTR currents showed time-dependent decreases and increases, respectively (Figure 5E). The kinetics fitted well to single exponential functions with time constants in the range 100–200 ms, substantially greater than those for GlyH-101 (8–10 ms) (Muanprasat et al., 2004), although comparable to those of MalH-lectin conjugates (Sonawane et al., 2007). The time constants showed little voltage dependence, and, at some potentials, were significantly greater for the monovalent versus the divalent conjugates
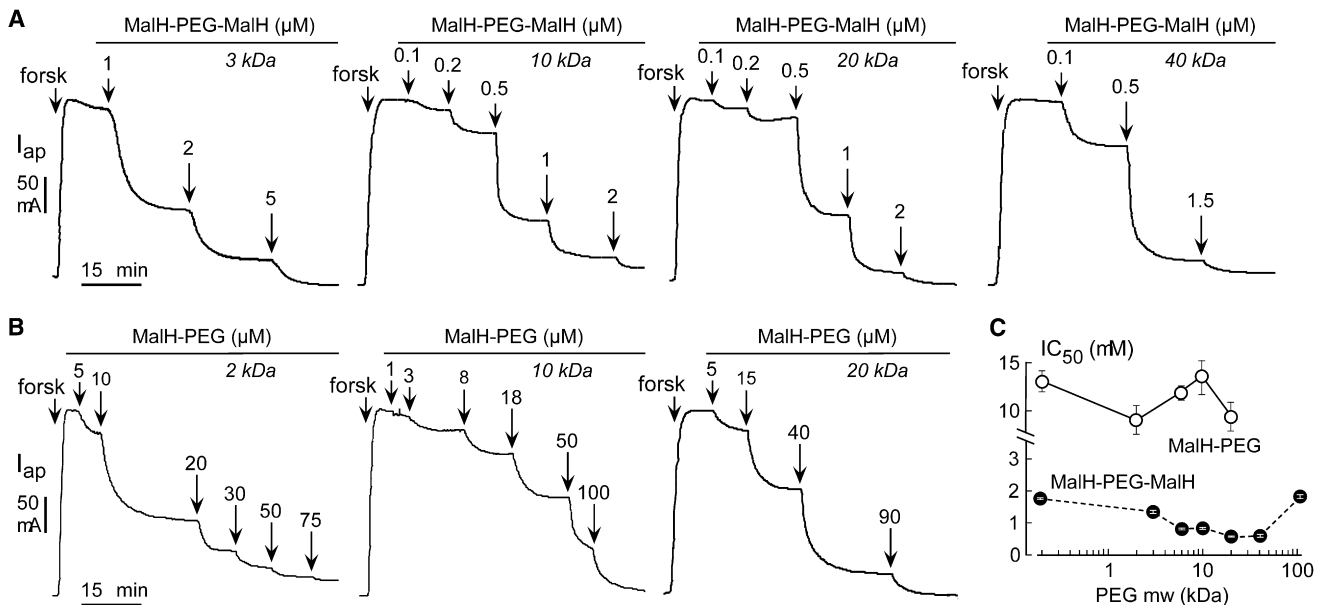
Figure 4. Short-Circuit Current Measurements of CFTR Inhibition

CFTR-mediated apical membrane chloride current measured in FRT cells expressing human wild-type CFTR after permeabilization of the basolateral membrane in the presence of a chloride gradient (see Experimental Procedures). CFTR was activated by 20 μM forskolin, and indicated concentrations of divalent MalH-PEG-MalH (A) and monovalent MalH-PEG (B) conjugates were added to apical bathing solution. (C) Deduced IC_{50} values. Error bars represent ± SE (n = 3–5).

(Figure 5F). As further evidence that the MalH-PEG conjugates act by a pore occlusion mechanism, lowering extracellular Cl⁻ to 20 mM strongly reduced the block by MalH-PEG-MalH (Figure 5G).

We estimated the distance of the MalH binding site along the electric field with the Woodhull equation (Woodhull, 1973). Assuming a valence (z) value of −1 for both monovalent and divalent compounds, the computed fraction of the membrane potential sensed at the binding site relative to the extracellular surface (δ) is 0.21 and 0.33, respectively. If z is −2 for the divalent compound, δ becomes 0.17.

Outside-out patch-clamp measurements were carried out to further investigate the mechanism of CFTR inhibition by the MalH-PEG conjugates. To activate CFTR, the pipette (intracellular) solution contained 1 mM ATP and 5 μg/ml protein kinase A catalytic subunit. Figures 6A and 6B show representative recordings of CFTR channel activity obtained at 60 mV in the absence and presence of divalent and monovalent conjugates. Compound addition to the extracellular side greatly reduced the duration of channel openings. Data from multiple experiments are summarized in Figures 6C and 6D. The MalH-PEG conjugates significantly reduced apparent mean open time and open channel probability. Apparent mean closed time was significantly reduced by the monovalent MalH-PEG. This effect is probably due to an increased number of brief intraburst closures, although the prevalence of multichannel patches in our experiments precluded a more detailed analysis of possible multicomponent channel closures in the presence of inhibitors. We also observed a small (∼10%) but significant decrease in single-channel amplitude (i). These results support the conclusion that MalH-PEG conjugates inhibit CFTR by an external pore occlusion mechanism (see Discussion).

Divalent MalH-PEG-MalH Conjugates Inhibit Cholera Toxin-Induced Intestinal Fluid Secretion

Inhibition efficacy of divalent conjugates was investigated in T84 colonic epithelial cells under nonpermeabilized conditions and in the absence of a Cl⁻ gradient. CFTR was activated by forskolin, and then MalH-PEG conjugates were added to the chamber bathing the apical cell surface. Figure 7A shows inhibition of forskolin-stimulated short-circuit current by 20 and 40 kDa MalH-PEG-MalH in T84 cells with IC_{50} values ∼1 μM.

The divalent MalH-PEG-MalH conjugates were tested for their antisecretory efficacy in mice in both intestinal closed-loop and suckling mouse survival models. Midjejunal loops were injected with either saline or cholera toxin containing different concentrations of test compounds, and intestinal fluid secretion was measured at 6 hr. Figure 7B shows a loop weight-to-length ratio of 0.06 g/cm in PBS-injected loops (corresponding to 100% inhibition), and ∼0.22 g/cm for cholera toxin-injected loops (corresponding to 0% inhibition). The divalent MalH-CFTR conjugates of 2, 10, 20, and 40 kDa molecular sizes inhibited cholera toxin-induced fluid secretion in a concentration-dependent manner, with IC_{50} values of ∼100, 10, 10, and 100 pmol/loop, respectively. PEG alone (bar at right) did not inhibit intestinal fluid accumulation.

Figure 7C summarizes the suckling mouse survival studies. Suckling 3–4 day-old Balb-C mice receiving a single oral dose of cholera toxin generally died by 20 hr, with no mortality in vehicle control (saline gavaged) mice over >24 hr. Survival of mice receiving cholera toxin was significantly improved when the divalent conjugate was gavaged along with cholera toxin. However, the survival of the inhibitor-treated mice was not 100%, which may have resulted from several factors, including imperfect inhibitor retention, intestinal distribution, and CFTR
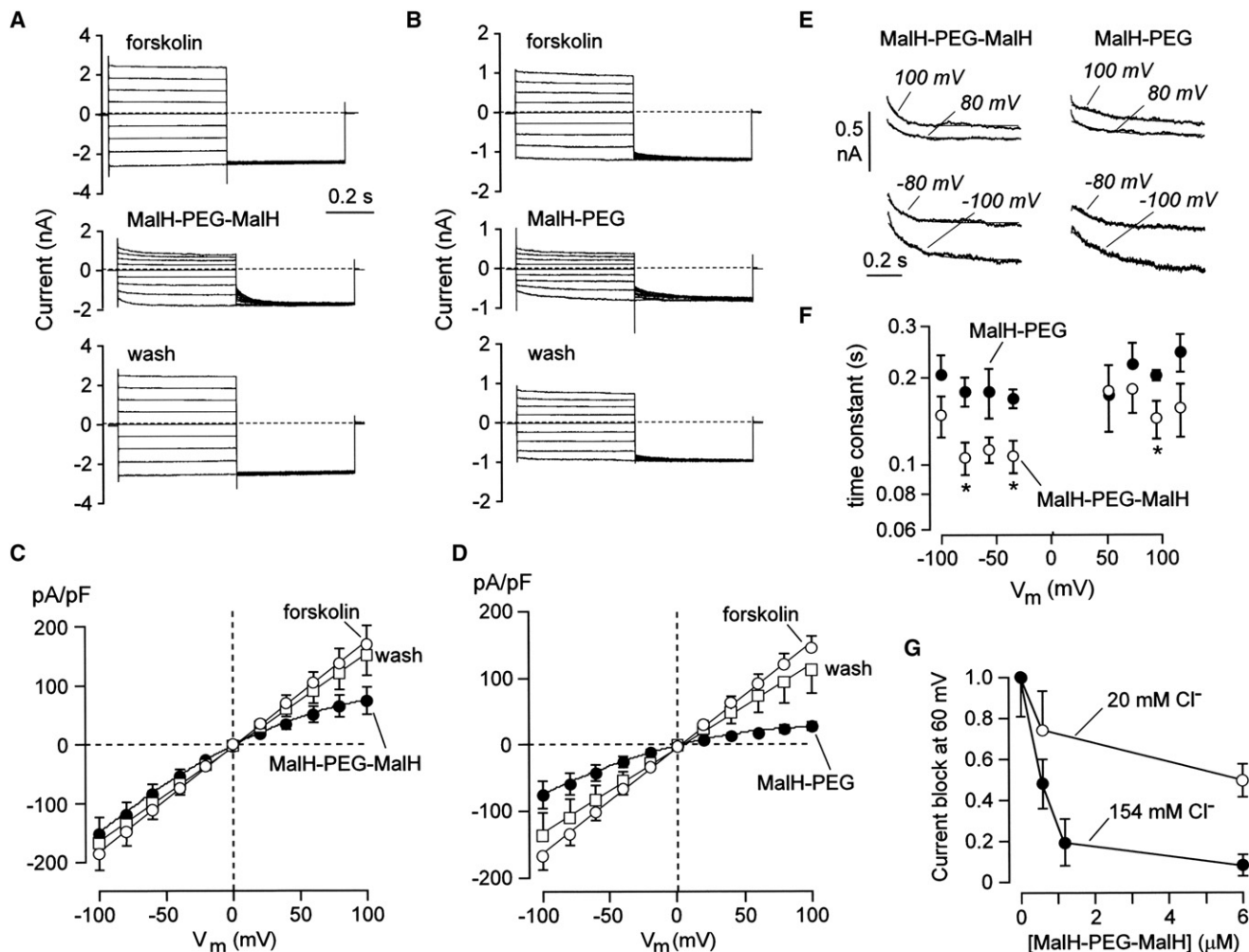
Figure 5. Electrophysiological Analysis of CFTR Inhibition by 20 kDa Conjugates

(A and B) Representative whole-cell membrane currents from CFTR-expressing FRT cells. Each panel shows superimposed membrane currents induced at different membrane potentials (from −100 to +100 mV) in 20 mV steps of 600 ms duration. Each pulse was followed by a 600 ms step at −100 mV. The interpulse interval was 4 s. Currents were measured before (upper panels), during (middle panels), and after (lower panels) application of the conjugates (0.6 μM for MalH-PEG-MalH; 15 μM for MalH-PEG). Forskolin (5 μM) was present throughout all measurements.

(C and D) Current-voltage relationships from whole-cell experiments as in (A) and (B). The current amplitude was reported as an average value at the end (550–600 ms) of the pulse, normalized to cell capacitance. Each point is the average. Error bars represent ± SE (four to five experiments). The inhibitors significantly reduced ($p < 0.05$) membrane current at voltages between 60 and 100 mV for MalH-PEG-MalH, and at all voltages, except 0 mV, for MalH-PEG.

(E) Kinetics of current relaxations elicited at indicated membrane voltages. Single exponential regressions are shown.

(F) Time constants measured at the indicated membrane voltages (Vm) by single exponential regression of current relaxations. Error bars represent ± SE (four to five experiments; *$p < 0.05$). Concentrations were 0.6 μM for MalH-PEG-MalH and 15 μM for MalH-PEG.

(G) Effect of extracellular Cl$^−$ concentration on MalH-PEG-MalH block. Inhibition of CFTR current measured at 60 mV in the presence of 154 or 20 mM extracellular Cl$^−$. Symbols are the mean of three to five different experiments. Error bars represent ± SE (*$p < 0.05$).

inhibition, as well as cholera toxin-related inhibition of intestinal fluid absorption.

DISCUSSION

Our study builds on a body of data on the discovery, external pore occlusion mechanism, and structure-activity relationship analysis of GlyH-type CFTR inhibitors, and their efficacy in blocking enterotoxin-mediated intestinal fluid secretion. The goal here was to develop nonabsorbable, potent CFTR inhibitors, which, unlike lectin conjugates (Sonawane et al., 2007), would be inex-

pensive, chemically stable, and nonimmunogenic. PEGs have been used extensively (at high concentrations) as laxatives in humans, and have an excellent safety profile (Migeon-Duballet et al., 2006). We found that conjugation of MalH CFTR-blocking moieties to a PEG backbone renders the MalH-PEG conjugate membrane impermeant and nonabsorbable, yet allows MalH access to its CFTR-blocking site at the extracellular surface of the CFTR anion pore. To improve the potency of prior GlyH analogs and conjugates, which had IC$_{50}$ values of 5 μM or greater (Muanprasat et al., 2004), we tested a series of multivalent CFTR blocker conjugates to PEGs, dextrans, dendrimers, and various
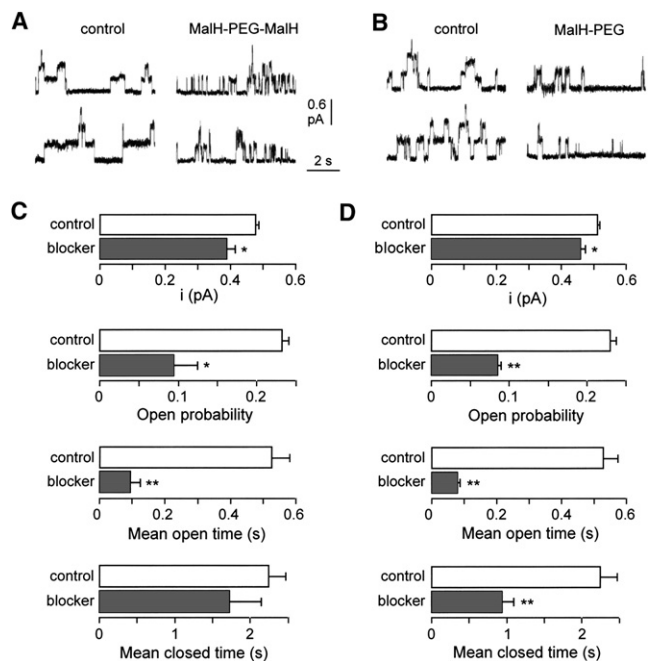
Figure 6. Outside-Out Patch-Clamp Recordings of CFTR Inhibition by MalH-PEG Conjugates

(A and B) Representative traces recorded at 60 mV showing CFTR single channel activity in the absence and presence of 20 kDa divalent and monovalent conjugates (2 and 15 μM, respectively). Pipette (intracellular) solution contained 1 mM ATP and 5 μg/ml protein kinase A catalytic subunit. Channel openings shown as upward deflections from the closed channel level (lowest currents).

(C and D) Summary of single-channel analysis for divalent and monovalent 20 kDa MalH-PEGs. Error bars represent 1 SE (four experiments; *p < 0.05; **p < 0.01).
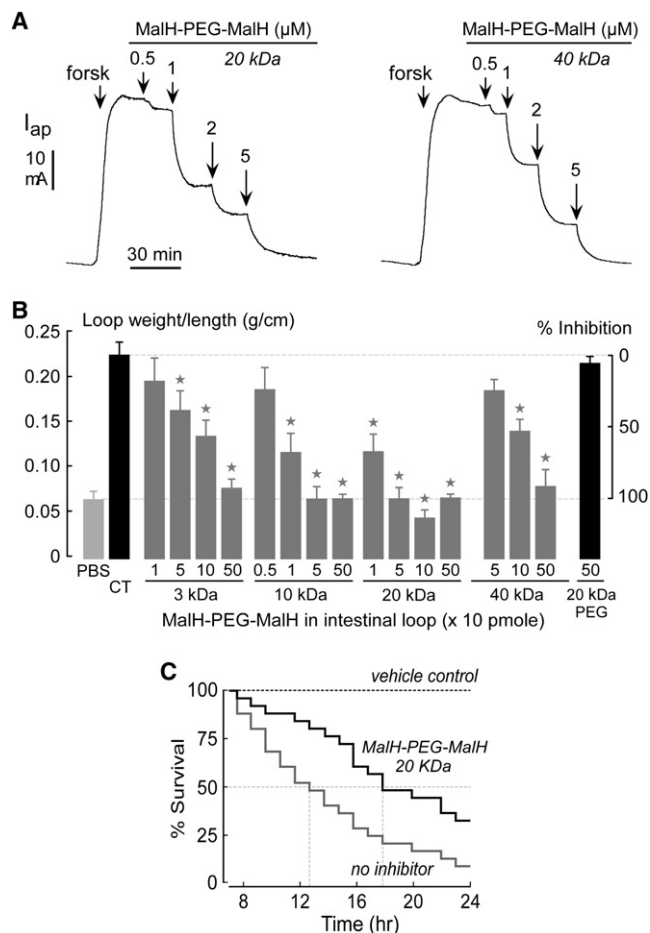

Figure 7. Antidiarrheal Efficacy of Divalent MalH-PEG-MalH Conjugates

(A) Inhibition of CFTR stimulated short-circuit current in human intestinal T84 cells (nonpermeabilized) by 20 and 40 kDa MalH-PEG-MalH. Data are representative of three sets of experiments. Where indicated, forskolin (20 μM) was added to activate CFTR. Baseline current was 3–7 μA.

(B) Intestinal fluid accumulation at 6 h, quantified by intestinal loop weight-to-length ratio, in closed midjejunal loops in mice. Error bars represent 1 SE (six to eight loops studied per condition; *p < 0.05, ANOVA).

(C) Improved survival of suckling mice (32 mice per group) following gavage with cholera toxin without versus with 200 pmol of 20 kDa MalH-PEG-MalH (p = 0.026, log-rank test). In vehicle control, mice were identically processed, but did not receive cholera toxin or inhibitors.

lipids, as well as different linker strategies. We found that divalent PEGs, containing MalH CFTR-blocking moieties at their termini, generally had >20-fold-improved potency for CFTR inhibition over monovalent conjugates, and had the requisite properties mentioned above for antidiarrheal applications. The greatly enhanced potency of divalent versus monovalent MalH-PEGs, and the relatively poor efficacy of the various other conjugates, could not be predicted in advance.

Experiments were done to investigate the mechanism of the greatly improved potency of divalent versus monovalent MalH-PEGs. The ∼2-fold-greater Hill coefficient for CFTR inhibition by divalent versus monovalent conjugates suggested cooperativity in binding as a key element in their improved potency, which could result from simultaneous two-site binding, or to various diffusion-concentration mechanisms whereby multivalency results in increased local concentration (Gestwicki et al., 2002). Simultaneous two-site binding would predict strongly size-dependent potency (Kramer and Karpen, 1998), in which the potency would be abruptly and strongly increased as the inter-MalH spacing exceeds the distance between binding sites on two CFTR monomers. This was not the case. The substantially greater potency of divalent versus monovalent MalH-PEGs for all size PEGs, even for very small PEGs of <200 Da (predicted solution length, ∼0.97 nm), excludes this possibility, as the pore-

pore separation between CFTR monomers is unlikely to be less than ∼11 nm (Rosenberg et al., 2004; Riordan, 2005; Guggino and Stanton, 2006). Our data thus suggest that the relatively high CFTR inhibition potency of the divalent MalH-PEGs is a consequence of the increased concentration at the external CFTR pore afforded by one-site/two-ligand binding.

Patch-clamp analysis indicated that the MalH-PEGs block CFTR chloride channel function in a voltage-dependent manner, similar to that found for unconjugated GlyH-101. In whole-cell patch-clamp recordings, inhibition by the divalent and monovalent conjugates was increased and reduced at positive and negative membrane potentials, respectively, and modulated by extracellular Cl⁻ concentration. This behavior supports the

conclusion that the negatively charged blocking moiety enters the CFTR pore from the extracellular side, and interacts at a site within the pore in which the blocker is sensitive to transmembrane electrical potential. Through the use of the Woodhull equation, the MalH-PEG conjugates appear to bind to a relatively shallow site (δ = 0.2–0.3), in agreement with CFTR pore models that postulate an asymmetric organization, with a deep and wide intracellular vestibule and a shorter extracellular access (Hwang and Sheppard, 1999; McCarty, 2000). Other CFTR blockers, including glibenclamide and disulfonic stilbenes, bind to the intracellular site of the pore and sense a higher fraction of transmembrane electrical field (δ = 0.4–0.5) (McCarty et al., 1993; Linsdell and Hanrahan, 1996; Sheppard and Robinson, 1997). We calculated δ for MalH-PEG-MalH for a z of −1 or −2, although we think that −1 is more appropriate. Although MalH-PEG-MalH has a net charge of −2, the two charges are located on opposite ends of PEG molecule, so that it is unlikely that both charges enter the same pore unless the molecule is tightly coiled and the charges are close to each other.

Outside-out patch-clamp recordings confirmed an external pore occlusion mechanism for CFTR inhibition by the MalH-PEG conjugates. The MalH-PEG conjugates affected primarily the channel open state, decreasing apparent mean open time. The time course of channel block and unblock in response to changes in membrane voltage, as measured in whole-cell recordings, showed single exponential behavior. A more complex mechanism, involving multiple steps with different time constants, would have produced multicomponent kinetics. The single time constants describing the kinetics of channel block and unblock were much greater than those of unconjugated GlyH-101, but comparable to those of the lectin conjugates. Also, in contrast to steady-state currents, the kinetics of block and unblock showed little voltage dependence, suggesting a high-energy, rate-limiting barrier that slows blocker entry and exit. From these findings, we postulate that conjugation reduces the mobility of the MalH pore-blocking moiety because of frictional interactions of the PEG chain within CFTR channel walls. Previous studies have evidenced the importance of such interactions in the mobility of linear macromolecules crossing transmembrane channels (Mathe et al., 2005).

Two mouse models of cholera were used to test the antisecretory properties of the divalent MalH-PEGs. The closed-loop model quantifies the accumulation of fluid in midjejunal loops in response to cholera toxin. This is a well-established and technically simple quantitative model in which fluid secretion and absorption mechanisms are intact, although there is no intestinal transit (Oi et al., 2002). Unfortunately, other than primates and surgically manipulated rabbits, suitable animal models of human-like secretory diarrheas are not available. As used here, the suckling mouse model, in which survival is the endpoint for intestinal fluid loss, is a reasonable model of cholera, although it does not accurately recapitulate human intestinal size, transit times, and fluid absorption/secretion rates (Takeda et al., 1978; Sonawane et al., 2007). Notwithstanding these caveats, the antisecretory potency of the divalent conjugates provides proof of concept for their antidiarrheal efficacy in vivo.

In summary, we have synthesized and characterized nonabsorbable, divalent MalH-PEG conjugates with nanomolar CFTR inhibition potency, which are effective in blocking cholera toxin-induced intestinal fluid secretion in mouse models of cholera. The safety, high potency, low cost, and chemical stability of these conjugates offer advantages over existing pore-blocking CFTR inhibitors, making them potential lead candidates for further preclinical development.

SIGNIFICANCE

Secretory diarrheas, such as cholera and traveler's diarrhea, are major health problems in developing countries. The current therapy—oral replacement of fluid losses—is primarily supportive. Oral replacement therapy has limited efficacy in the very young and old, and when clean water and "oral rehydration salt" mixture is not available. Therapy directed at reducing intestinal fluid secretion (antisecretory therapy) has the potential to overcome limitations of existing therapies. The cystic fibrosis chloride channel (CFTR) is the main pathway involved in fluid secretion in secretory diarrheas. Because CFTR is expressed at the luminal membrane of intestinal epithelial cells (enterocytes), it represents a unique target for development of an orally administered, nonabsorbable CFTR inhibitor. We report the development of such an inhibitor, which involved conjugation of a CFTR pore-blocking moiety (MalH) with a polyethylene glycol (PEG) macromolecular backbone. PEGs are safe and render the CFTR inhibitor nonabsorbable. We discovered greatly enhanced potency by linking two MalH moieties to opposite ends of one PEG. The macromolecular CFTR inhibitors are shown by patch-clamp analysis to block CFTR by an external pore occlusion mechanism, and are found to effectively block intestinal fluid secretion in mouse models of cholera. Because of their high potency, chemical stability, and membrane impermeability, the MalH-PEG conjugates developed in this study have potential application as safe oral antisecretory therapy in cholera and traveler's diarrhea.

EXPERIMENTAL PROCEDURES

Synthesis Procedures
^{1}H and ^{13}C NMR spectra were obtained in CDCl$_3$ or DMSO-d$_6$ with a 400 MHz Varian Spectrometer referenced to CDCl$_3$ or DMSO. Mass spectrometry was performed on a Waters LC/MS system (Alliance HT 2790+ZQ, HPLC; model 2690; Waters, Milford, MA). Flash chromatography was performed with EM silica gel (230–400 mesh), and thin-layer chromatography was performed on Merk silica gel 60 F254 plates.

MalH-PEG-MalH and MalH-PEG, General Procedure
Bisamino or mono-amino PEGs (0.25, 1, 2, 3, 6, 10, 20 kDa; Sigma; 40 and 100 kDa synthesized as described below) (each 20 mg in 0.5 ml DMSO), MalH-DIDS (5 molar excess; Sonawane et al., 2007), and triethylamine (5-fold molar excess) were stirred slowly at room temperature for 1 hr. Amino-functionalized silica gel (10-fold molar excess) was added and stirred for an additional 2 hr. The reaction mixture was filtered, scavenger was washed with 1 ml DMSO, and the combined filtrate was added dropwise with stirring into 50 ml methanol. The precipitated product was filtered and washed twice with methanol. PEG conjugates of 6 kDa size and lower were further purified by anion exchange chromatography (sepharose; GE) with NaCl gradient (0.5–1.0 M) elution. PEG conjugates of 10, 20, 40, and 100 kDa sizes were dialyzed by overnight dialysis against PBS. Larger PEG conjugates were purified by gel filtration (sephadex G25).

MalH-PEG0.1kDa-OH: yield, 49%; mp > 300°C; ^{1}H NMR (D$_2$O): δ 3.19−4.44 (s, 8H, PEG-CH$_2$), 4.72, 5.22 (d, m, ∼1H, COCH), 7.60–7.88 (m, Ar-H), MS (ES$^-$)

(m/z): $[M-2H]^{2-}$ and $[M-1]^-$ calculated for $C_{40}H_{38}Br_2N_8O_{11}S_4$, 546.43 and 1094.86, found 545, 546, 547 $[M-2H]^{2-}$, 1091, 1093, 1095 $[M-H]^-$.

MalH-PEG0.75kDa-OMe: yield, 18%; ^1H NMR (D_2O): δ, 2.85 (s, OCH_3), 3.52 (s, PEG-CH_2), 7.60–7.82 (m, Ar-H), MS (ES$^+$) (m/z): ($[M]^+$+Na$^+$)/2 calculated for $C_{69}H_{96}Br_2N_8O_{25}S_4$, 896.31, found 896 ± 22, 44, 88, 176 (Figure 2B).

MalH-PEG2kDa-OMe: yield 31%; ^1H NMR (D_2O): δ, 2.69 (s, O-CH_3), 3.21 (s, PEG-CH_2), 7.57–7.90 (m, Ar-H), MS (ES$^+$) (m/z): $[M-2H]^{2-}$ calculated for $C_{121}H_{200}Br_2N_8O_{51}S_4$, 1433.0, found 1432.8 ± 22, 44, 88, 176 (Figure 2B).

MalH-PEG5kDa-OMe: yield 53%; ^1H NMR (D_2O): δ, 2.64 (s, O-CH_3), 3.50 (s, PEG-CH_2), 7.38–7.91 (m, Ar-H); Conjugation ratio, MalH:PEG 1: 1.04 (UV/Visible).

MalH-PEG10kDa-OMe: yield 62%; ^1H NMR (D_2O): δ, 2.58 (s, O-CH_3), 3.49 (s, PEG-CH_2), 7.55–8.07 (m, Ar-H); Conjugation ratio, MalH:PEG 1: 1.08 (UV/Visible).

MalH-PEG20kDa-OMe: yield 39%; ^1H NMR (D_2O): δ, 2.59 (s, O-CH_3), 3.48 (s, PEG-CH_2), 7.40–7.96 (m, Ar-H); Conjugation ratio, MalH:PEG 1: 0.96 (UV/Visible).

MalH-PEG0.14kDa-MalH: yield 29%; ^1H NMR (D_2O): δ, 3.21–3.60 (m, PEG-CH_2), 3.62–3.71 (m, PEG-CH_2), 7.27–7.82 (m, Ar-H), MS (ES$^+$) (m/z): $[M-2H]^{2-}$ and ($[M-2H]^{2-}$ 3Na$^+$) calculated for $C_{78}H_{70}Br_4N_{16}O_{20}S_8$, 1062.82 and 1131.82, found 1062.94 and 1130.88.

MalH-PEG3kDa-MalH: yield 44%; ^1H NMR (D_2O): δ, 3.48 (s, PEG-CH_2), 7.13–780 (m, Ar-H), MS (ES$^+$) (m/z): $[[M-4H]^{4-}$+ Na$^+$]/4 calculated for $C_{224}H_{362}Br_4N_{16}O_{93}S_8$, 1339.25, found 1339 (Figure 2B).

MalH-PEG6kDa-MalH: yield 26%; ^1H NMR (D_2O): δ, 3.51 (s, PEG-CH_2), 7.22–8.14 (m, Ar-H); conjugation ratio, MalH:PEG 2: 1.11 (UV/Visible).

MalH-PEG10kDa-MalH: yield 23%; ^1H NMR (D_2O): δ, 3.46 (s, PEG-CH_2), 7.05–8.21 (m, Ar-H); conjugation ratio, MalH:PEG 2: 0.92 (UV/Visible).

MalH-PEG20kDa-MalH: yield 55%; ^1H NMR (D_2O): δ, 3.53 (s, PEG-CH_2), 7.14–7.91 (m, Ar-H); conjugation ratio, MalH:PEG 2: 1.07 (UV/Visible).

MalH-PEG40kDa-MalH: yield 27%; ^1H NMR (D_2O): δ, 3.53 (s, PEG-CH_2), 7.13–8.12 (m, Ar-H); conjugation ratio, MalH:PEG 2: 0.95 (UV/Visible).

MalH-PEG108kDa-MalH: yield 58%; ^1H NMR (D_2O): δ, 3.60 (s, PEG-CH_2), 7.07–7.89 (m, Ar-H); conjugation ratio, MalH:PEG 2: 1.08 (UV/Visible).

Bisamino-PEGs, 40 and 100 kDa

To a mixture of PEG (25 μmol, 40 and 108 kDa; Sigma) and triethylamine (14 μl, 100 μmol) in 2–5 ml CH_2Cl_2, methane sulfonyl chloride (52 mmol) was added dropwise at 0°C and stirred for 6 hr at room temperature. The reaction mixture was washed with sodium bicarbonate (50 mM, 2 ml) and the organic phase was dried ($MgSO_4$). The evaporated organic phase yielded 1,w-dimethanesulfonylpolyoxyethylenes of 40 and 100 kDa, which were dissolved in 2 ml DMSO, and NaN_3 (13 mg, 0.2 mmol) was added and stirred for 6 hr at 50°C. After cooling, water (20 ml) was added, and the PEG-azide was extracted in dichloromethane and evaporated. A mixture of the PEG-azide (10 μmol) and triphenylphosphine (8 mg, 30 μmol) in dry methanol (3 ml) was refluxed for 1 hr and solvent was removed under reduced pressure. The residue was dissolved in dichloromethane (10 ml), filtered, and then exposed to dry hydrogen chloride gas. The precipitated hydrochloride salt of bisamino PEG was filtered. The solution was cooled at 4°C overnight, and the precipitated hydrogen chloride salt was further purified by cation exchange chromatography with carboxymethyl CM-sephadex C25, eluted with 10 mM Tris, pH 9.0, and a 2 L gradient of 0.1–2.0 M NaCl. H_2N-PEG 40 kDa-NH_2: 26% yield, ^1H NMR (D_2O): δ, 2.91 (m, -CH_2-N), 3.27 (t, O-CH_2-C-N), 3.52 (s, PEG-CH_2). H_2N-PEG108kDa-NH_2: 38% yield, ^1H NMR (D_2O): δ, 2.90 (m, -CH_2-N), 3.31 (t, O-CH_2-C-N), 3.51 (s, PEG-CH_2).

Fluorescence Cell-Based Assay of CFTR Inhibition

Fisher rat thyroid (FRT) cells stably expressing wild-type human CFTR and YFP-H148Q were cultured on 96 well black-wall plates, as previously described (Ma et al., 2002). Cells in 96 well plates were washed three times, and then CFTR was activated by incubation for 15 min with an activating cocktail containing 10 μM forskolin, 20 μM apigenin, and 100 μM IBMX. Test compounds were added 5 min before assay of iodide influx in which cells were exposed to a 100 mM inwardly directed iodide gradient. YFP fluorescence was recorded for 2 s before and 12 s after creation of the iodide gradient. Initial rates of iodide influx were computed from the time course of decreasing fluorescence after the iodide gradient.

Short-Circuit Current Measurements

FRT cells (stably expressing human wild-type CFTR) were cultured on Snapwell filters with 1 cm^2 surface area (Corning-Costar) to resistance of >1,000 Ω · cm^2, as previously described (Sonawane et al., 2007). Filters were mounted in an Easymount Chamber System (Physiologic Instruments, San Diego, CA). For apical Cl$^-$ current measurements, the basolateral hemichamber contained: 130 mM NaCl, 2.7 mM KCl, 1.5 mM KH_2PO_4, 1 mM $CaCl_2$, 0.5 mM $MgCl_2$, 10 mM Na-HEPES, 10 mM glucose (pH 7.3). The basolateral membrane was permeabilized with amphotericin B (250 μg/ml) for 30 min. In the apical solution 65 mM NaCl was replaced by sodium gluconate, and $CaCl_2$ was increased to 2 mM to compensate for Ca^{2+} buffering by gluconate. The basolateral-to-apical Cl$^-$ gradient induces upward current deflections, indicating flow of Cl$^-$ from the basolateral to the apical side of the epithelium. Solutions were bubbled with 95% O_2/5% CO_2 and maintained at 37°C. Current was recorded with a DVC-1000 voltage clamp (World Precision Instruments) with Ag/AgCl electrodes and 1 M KCl agar bridges.

Closed Intestinal Loop Model of Cholera

Mice (CD1 strain, 28–34 g) were given 5% sucrose for 24 hr prior to anesthesia (2.5% avertin intraperitoneally). Body temperature was maintained at 36°C–38°C with a heating pad. Following a small abdominal incision, three or four closed midjejunal loops (length, 15–20 mm) were isolated by sutures. Loops were injected with 100 μl PBS or PBS containing cholera toxin (1 μg), without or with test compounds. The abdominal incision was closed with sutures, and the mice were allowed to recover from anesthesia. At 6 hr, the mice were again anesthetized, the intestinal loops were removed, and loop length and weight were measured to quantify net fluid accumulation. Mice were killed by an overdose of avertin. All protocols were approved by the UCSF Committee on Animal Research.

Suckling Mouse Model of Cholera

Equal numbers of newborn Balb-C mice from the same mother(s), each weighing 2–3 g (age 3–4 days), were gavaged with PE-10 tubing with 10 μg cholera toxin in a 50 μl volume containing 50 mM Tris, 200 mM NaCl, and 0.08% Evans blue (pH 7.5), with or without MalH-PEG 20 kDa-MalH (5 nmol). Control mice were gavaged with buffer alone. Successful gavage was confirmed by Evans blue localization in stomach/intestine. Mouse survival was assessed hourly.

Patch-Clamp Analysis

Patch-clamp experiments were carried out at room temperature on FRT cells stably expressing wild-type CFTR. Whole-cell and outside-out configurations were used. For whole-cell experiments, the pipette solution contained: 120 mM CsCl, 10 mM TEA-Cl, 0.5 mM EGTA, 1 mM $MgCl_2$, 40 mM mannitol, 10 mM Cs-HEPES, and 1 mM MgATP (pH 7.3). For outside-out patches, the pipette solution contained: 150 mM NMDG-Cl, 2 mM $MgCl_2$, 10 mM EGTA, 10 mM HEPES, 1 mM ATP (pH 7.3). This pipette solution was supplemented with 125 nM catalytic subunit of protein kinase A (Promega). The stock solution of the catalytic subunit of protein kinase A was further diluted up to 250 mg/ml in a buffer containing dithiothreitol and aliquots were kept at −80°C. After thawing, aliquots were maintained at 4°C for not more than 2 weeks. The bath solution in all experiments was: 150 mM NaCl, 1 mM $CaCl_2$, 1 mM $MgCl_2$, 10 mM glucose, 10 mM mannitol, 10 mM Na-HEPES (pH 7.4). The cell membrane was clamped at specified voltages with an EPC-7 patch-clamp amplifier (List Medical). Data were filtered at 500 Hz (whole cell) or 200 Hz (outside-out), and digitized at 1,000 Hz with an Instrutech ITC-16 AD/DA interface and PULSE software (Heka). Mean cell capacitance was 17.8 ± 1.6 pF (n = 19). Inhibitors were applied by extracellular perfusion. Whole-cell and single-channel recordings were analyzed with IgorPro software (Wavemetrics) and custom procedures. In the outside-out configuration, most membrane patches contained several channels (three to nine), precluding dwell time analysis and determination of dwell time constants for open and closed channel states. Therefore, blocker effects were described by mean open and closed times.

REFERENCES

Baird, E.J., Holowka, D., Coates, G.W., and Baird, B. (2003). Highly effective poly(ethylene glycol) architectures for specific inhibition of immune receptor activation. Biochemistry 42, 12739–12748.

Barrett, K.E., and Keely, S.J. (2000). Chloride secretion by the intestinal epithelium: molecular basis and regulatory aspects. Annu. Rev. Physiol. 62, 535–572.

Boucher, R.C. (2004). New concepts of the pathogenesis of cystic fibrosis lung disease. Eur. Respir. J. 23, 146–158.

Clarke, L.L., Grubb, B.R., Gabriel, S.E., Smithies, O., Koller, B.H., and Boucher, R.C. (1992). Defective epithelial chloride transport in a gene-targeted mouse model of cystic fibrosis. Science 257, 1125–1128.

Field, M. (2003). Intestinal ion transport and the pathophysiology of diarrhea. J. Clin. Invest. 111, 931–943.

Gabriel, S.E., Brigman, K.N., Koller, B.H., Boucher, R.C., and Stutts, M.J. (1994). Cystic fibrosis heterozygote resistance to cholera toxin in the cystic fibrosis mouse model. Science 266, 107–109.

Galietta, L.J.V., Jayaraman, S., and Verkman, A.S. (2001). Cell-based assay for high-throughput quantitative screening of CFTR chloride transport agonists. Am. J. Physiol. 281, C1734–C1742.

Gestwicki, J.E., Cairo, C.W., Strong, L.E., Oetjen, K.A., and Kiessling, L.L. (2002). Influencing receptor-ligand binding mechanisms with multivalent ligand architecture. J. Am. Chem. Soc. 124, 14922–14933.

Guggino, W.B., and Stanton, B.A. (2006). New insights into cystic fibrosis: molecular switches that regulate CFTR. Nat. Rev. Mol. Cell Biol. 7, 426–436.

Handl, H.L., Sankaranarayanan, R., Josan, J.S., Vagner, J., Mash, E.A., Gillies, R.J., and Hruby, V.J. (2007). Synthesis and evaluation of bivalent NDP-α-MSH(7) peptide ligands for binding to the human melanocortin receptor 4 (hMC4R). Bioconjug. Chem. 18, 1101–1109.

Hwang, T.C., and Sheppard, D.N. (1999). Molecular pharmacology of the CFTR Cl⁻ channel. Trends Pharmacol. Sci. 20, 448–453.

Kramer, R.H., and Karpen, J.W. (1998). Spanning binding sites on allosteric proteins with polymer-linked ligand dimers. Nature 395, 710–713.

Krouse, M.E., and Wine, J.J. (2001). Evidence that CFTR channels can regulate the open duration of other CFTR channels: cooperativity. J. Membr. Biol. 182, 223–232.

Kunzelmann, K., and Mall, M. (2002). Electrolyte transport in the mammalian colon: mechanisms and implications for disease. Physiol. Rev. 82, 245–289.

Linsdell, P., and Hanrahan, J.W. (1996). Disulphonic stilbene block of cystic fibrosis transmembrane conductance regulator Cl⁻ channels expressed in a mammalian cell line and its regulation by a critical pore residue. J. Physiol. 496, 687–693.

Li, H., Findlay, I.A., and Sheppard, D.N. (2004). The relationship between cell proliferation, Cl⁻ secretion, and renal cyst growth: a study using CFTR inhibitors. Kidney Int. 66, 1926–1938.

Li, C., Dandridge, K.S., Di, A., Marrs, K.L., Harris, E.L., Roy, K., Jackson, J.S., Makarova, N.V., Fujiwara, Y., Farrar, P.L., et al. (2005). Lysophosphatidic acid inhibits cholera toxin-induced secretory diarrhea through CFTR-dependent protein interactions. J. Exp. Med. 202, 975–986.

Ma, T., Thiagarajah, J.R., Yang, H., Sonawane, N.D., Folli, C., Galietta, L.J., and Verkman, A.S. (2002). Thiazolidinone CFTR inhibitor identified by high-throughput screening blocks cholera toxin-induced intestinal fluid secretion. J. Clin. Invest. 110, 1651–1658.

Mathe, J., Aksimentiev, A., Nelson, D.R., Schulten, K., and Meller, A. (2005). Orientation discrimination of single-stranded DNA inside the α-hemolysin membrane channel. Proc. Natl. Acad. Sci. USA 102, 12377–12382.

McCarty, N.A. (2000). Permeation through the CFTR chloride channel. J. Exp. Biol. 203, 1947–1962.

McCarty, N.A., McDonough, S., Cohen, B.N., Riordan, J.R., Davidson, N., and Lester, H.A. (1993). Voltage-dependent block of the cystic fibrosis transmembrane conductance regulator Cl⁻ channel by two closely related arylamino-benzoates. J. Gen. Physiol. 102, 1–23.

Migeon-Duballet, I., Chabin, M., Gautier, A., Mistouflet, T., Bonnet, M., Aubert, J.M., and Halphen, M. (2006). Long-term efficacy and cost-effectiveness of polyethylene glycol 3350 plus electrolytes in chronic constipation: a retrospective study in a disabled population. Curr. Med. Res. Opin. 22, 1227–1235.

Muanprasat, C., Sonawane, N.D., Salinas, D., Taddei, A., Galietta, L.J., and Verkman, A.S. (2004). Discovery of glycine hydrazide pore-occluding CFTR inhibitors: mechanism, structure-activity analysis, and in vivo efficacy. J. Gen. Physiol. 124, 125–137.

Oi, H., Matsuura, D., Miyake, M., Ueno, M., Takai, I., Yamamoto, T., Kubo, M., Moss, J., and Noda, M. (2002). Identification in traditional herbal medications and confirmation by synthesis of factors that inhibit cholera toxin-induced fluid accumulation. Proc. Natl. Acad. Sci. USA 99, 3042–3046.

Pal, B., Jaisankar, P., and Giri, V.S. (2004). Versatile reagent for reduction of azides to amines. Synth. Commun. 34, 1317–1323.

Ramjeesingh, M., Kidd, J.F., Huan, L.J., Wang, Y., and Bear, C.E. (2003). Dimeric cystic fibrosis transmembrane conductance regulator exists in the plasma membrane. Biochem. J. 374, 793–797.

Riordan, J.R. (2005). Assembly of functional CFTR chloride channels. Annu. Rev. Physiol. 67, 701–718.

Rosenberg, M.F., Kamis, A.B., Aleksandrov, L.A., Ford, R.C., and Riordan, J.R. (2004). Purification and crystallization of the cystic fibrosis transmembrane conductance regulator (CFTR). J. Biol. Chem. 279, 39051–39057.

Routaboul, C., Norez, C., Melin, P., Molina, M.C., Boucherle, B., Bossard, F., Noel, S., Robert, R., Gauthier, C., Becq, F., and Décout, J.L. (2007). Discovery of alpha-aminoazaheterocycle-methylglyoxal adducts as a new class of high-affinity inhibitors of cystic fibrosis transmembrane conductance regulator chloride channels. J. Pharmacol. Exp. Ther. 322, 1023–1035.

Schillers, H., Shahin, V., Albermann, L., Schafer, C., and Oberleithner, H. (2004). Imaging CFTR: a tail to tail dimer with a central pore. Cell. Physiol. Biochem. 14, 1–10.

Sheppard, D.N., and Robinson, K.A. (1997). Mechanism of glibenclamide inhibition of cystic fibrosis transmembrane conductance regulator Cl⁻ channels expressed in a murine cell line. J. Physiol. 503, 333–346.

Sheppard, D.N., and Welsh, M.J. (1992). Effect of ATP-sensitive K⁺ channel regulators on cystic fibrosis transmembrane conductance regulator chloride currents. J. Gen. Physiol. 100, 573–591.

Sonawane, N.D., Muanprasat, C., Nagatani, R., Song, Y., and Verkman, A.S. (2005). In vivo pharmacology and antidiarrheal efficacy of a thiazolidinone CFTR inhibitor in rodents. J. Pharm. Sci. 94, 134–143.

Sonawane, N.D., Hu, J., Muanprasat, C., and Verkman, A.S. (2006). Luminally active, nonabsorbable CFTR inhibitors as potential therapy to reduce intestinal fluid loss in cholera. FASEB J. 20, 130–132.

Sonawane, N.D., Zhao, D., Zegarra-Moran, O., Galietta, L.J., and Verkman, A.S. (2007). Lectin conjugates as potent, nonabsorbable CFTR inhibitors for reducing intestinal fluid secretion in cholera. Gastroenterology 132, 1234–1244.

Sonawane, N.D., Zegarra-Moran, O., Namkung, W., Galietta, L.J., and Verkman, A.S. (2008). α-Aminoazaheterocyclic-methylglyoxal adducts do not inhibit cystic fibrosis transmembrane conductance regulator chloride channel activity. J. Pharmacol. Exp. Ther. 325, 529–535.

Staudinger, H., and Meyer, J. (1919). New organic compounds of phosphorus. III. Phosphinemethylene derivatives and phosphinimines. J. Helv. Chim. Acta. 2, 635–646.

Taddei, A., Folli, C., Zegarra-Moran, O., Fanen, P., Verkman, A.S., and Galietta, L.J. (2004). Altered channel gating mechanism for CFTR inhibition by a high-affinity thiazolidinone blocker. FEBS Lett. 558, 52–56.

Takeda, T., Takeda, Y., Miwatani, T., and Ohtomo, N. (1978). Detection of cholera enterotoxin activity in suckling hamsters. Infect. Immun. 19, 752–754.

Thiagarajah, J.R., and Verkman, A.S. (2005). New drug targets for cholera therapy. Trends Pharmacol. Sci. 26, 172–175.

Thiagarajah, J.R., Broadbent, T., Hsieh, E., and Verkman, A.S. (2003). Prevention of toxin-induced intestinal ion and fluid secretion by a small-molecule CFTR inhibitor. Gastroenterology 126, 511–519.

Walsh, K.B., Long, K.J., and Shen, X. (1999). Structural and ionic determinants of 5-nitro-2-(3-phenylprophyl-amino)-benzoic acid block of the CFTR chloride channel. Br. J. Pharmacol. 127, 369–376.

Wang, S., Yue, H., Derin, R.B., Guggino, W.B., and Li, M. (2000). Accessory protein facilitated CFTR-CFTR interaction, a molecular mechanism to potentiate the chloride channel activity. Cell 103, 169–179.

Woodhull, A.M. (1973). Ionic blockage of sodium channels in nerve. J. Gen. Physiol. 61, 687–708.

Yang, B., Sonawane, N.D., Zhao, D., Somlo, S., and Verkman, A.S. (2008). Small-molecule CFTR inhibitors slow cyst growth in culture and mouse models of polycystic kidney disease. J. Am. Soc. Nephrol. 19, 1300–1310.

Zerhusen, B., Zhao, J., Xie, J., Davis, P.B., and Ma, J. (1999). A single conductance pore for chloride ions formed by two cystic fibrosis transmembrane conductance regulator molecules. J. Biol. Chem. 274, 7627–7630.

Zhou, Z., Hu, S., and Hwang, T.C. (2002). Probing an open CFTR pore with organic anion blockers. J. Gen. Physiol. 120, 647–662.